Laser and Particle Beams (2010), *28*, 377–385.

doi:10.1017/S0263034610000327

Design of a dual-band power combining architecture for high-power microwave applications

QIANG ZHANG, CHENGWEI YUAN, AND LIE LIU

College of Optoelectronic Science and Engineering, National University of Defense Technology, Changsha, People's Republic of China

(RECEIVED 2 November 2009; ACCEPTED 1 May 2010)

Abstract

The remaining challenges, confronting the limited output peak power level of high-power microwave (HPM) sources, stimulate the development of power combining system. This paper reports the design methods and numerical results for a kind of dual-band incoherent power combining architecture applied in HPM. It is particularly effective to radiate dual-band microwave simultaneously, generated by a coaxial dual-band HPM source or two separate HPM sources of different bands. Two types of mode conversion structures, i.e., a dual-band feed line with co-aligned ports and a dual-band feed line with off-aligned ports, are proposed, where coaxial output port itself is adopted to connect the coaxial dual-band horn feed. These two types of feed lines provide a high conversion efficiency of about 98% from TEM or TM_{01} mode to TE_{11} mode and a bandwidth of about 10% at each band. The horn feed, with a high power handling capacity, is compact, and a good far-field radiation pattern at each band has been achieved by combining horizontal and vertical corrugations. Thus, the dual-band radiation system has not only realized incoherent power combination, with higher output peak power level, but also is suitable for feeding of, e.g., offset shaped single-reflector antennas in dual-band HPM systems in the future.

Keywords: Corrugated horn feed; Dual-band feed; High-power microwaves; Mode converters; Power combination; Simulation

INTRODUCTION

High power microwaves (HPMs) span a wide rage of applications in both civilian and military fields (Baker & Schamiloglu, 2001; Benford *et al.*, 2007). During recent years, based on the fast development of pulsed power technology (Liu *et al.*, 2006, 2007*a*, 2007*b*, 2008, 2009; Yatsui *et al.*, 2005; Zou *et al.*, 2006) and intense electron beam generation from conventional accelerators (Li *et al.*, 2009*a*, 2009*b*, 2009*c*), HPM technologies have achieved a significant progress, different HPM sources have been produced in the past two decades, and some of them have reached the power of gigawatt (GW) class (Eltchaninov *et al.*, 2003; Korovin *et al.*, 2003). However, the efforts to reach higher output peak power levels are increasing due to the rapid progress in HPM technology. On the other hand, the increasing demand for more transmission frequencies promotes the number of channels in the HPM systems, and HPM devices with several output frequencies become more and more attractive (Baker & Schamiloglu, 2001; Li *et al.*, 2008).

To meet the requirements mentioned above, it is an effective approach to obtain higher peak power microwave beam output while maintaining a good beam quality by combining multiple output microwaves from a number of HPM sources, working at different bands. Compared with incoherent combining, it is difficult to realize coherent combining for HPM applications, considering the effect of phase error, beam jitter, and some other nonlinear factors. In previous studies, power combination systems, i.e., circuit power combining have been used widely in low power levels, which cannot be utilized directly in HPM field, considering the power-handling capacity. Thus, to discriminate it from the circuit power combining, waveguide-based spatial power combining can be adopted to the solid-state inner space combining. In this paper, a new architecture for waveguide-based spatial dual-band power combining radiation system is discussed, using two types of feed lines and a compact horn feed.

As mentioned above, the architecture to be introduced determines whether HPM energy can be utilized effectively. Compared with the conventional techniques, this structure should focus on the two major points: first, transforming

Address correspondence and reprint requests to: Q. Zhang, College of Optoelectronic Science and Engineering, National University of Defense Technology, Changsha 410073, People's Republic of China. E-mail: zqiang1984@163.com

azimuthally symmetric modes into other modes that can be concentrated on the goal point effectively; second, realizing the high power-handling capacity.

The required geometry of the mode converter depends on the details of the two modes that are being interchanged. A dual-bend mode converter (Yang *et al.*, 1997) has been proposed to realize high conversion efficiency from TM_{01} to TE_{11} circular waveguide mode, which can be used in conventional systems directly. Another kind of TEM-TE_{11} mode converter (Yuan *et al.*, 2005) has also been investigated, which has a coaxial plate-inserted structure. It has the virtues of co-aligned ports, a compact structure, and easy manufacturing. However, the former may have a higher power-handling capacity, because it can be designed with oversized waveguides, while the coaxial plate-inserted TEM $-$ TE_{11} mode converter can not.

For most types of mode converters, they are mainly working effectively in a single band. However, dual- or multi-band power combining systems are often required extremely for many current applications, especially with the development of dual-band HPM technology. Dual- or multi-band power combining systems, with a high power handling capacity, have necessarily become one developing direction of antennas.

As early as the 1990s, a frequency selective horn (Vardaxoglou *et al.*, 1992) working at Ku/K band simultaneously has been designed successfully, utilizing frequency selective surfaces. The measured results show that the horn has the virtues of broad bandwidth and less weight. However, it has to be investigated further about the radiation characteristics determined by the design of frequency selective surfaces. Then, a dual-band corrugated horn antenna (Flodin *et al.*, 1996; Imbriale, 2005) has been investigated using moment method. However, the return loss cannot be ignored, and the structure is difficult to manufacture. Furthermore, the power handling capacity is not very high. The requirement for the HPM devices is low transmission loss at the power level of GW class. It is, therefore, necessary to redesign a new architecture, suitable for HPM applications.

In this paper, we will detail the design methods of dual-band power combining architecture, which comprises two parts, i.e., feed line structures and a corrugated dual-band horn feed. For the feed line structures, we will introduce two designed results: one is a dual-band feed line with co-aligned ports; another is a dual-band feed line with off-aligned input ports and coaxial output ports, realizing mode conversion from TM_{01} or TEM mode to TE_{11} mode effectively. The horn feed, based on the combination of horizontal and vertical corrugations, is proposed to meet the requirements of far-field radiation pattern at each band.

DESIGN OF FEED LINEE STRUCTURE

Dual-Band Feed Line with Co-Aligned Ports

Recently, NUDT of China has proposed a novel coaxial dual-band HPM source (Fan *et al.*, 2007; Zhang *et al.*, 2008), generating coaxial TEM mode at low band and TM_{01} mode at high band, respectively, as shown in Figure 1. It was investigated in detail with particle-in-cell methods (KARAT code), which are demonstrated by experiments. And experimental research shows that the microwave frequency generated by the dual-band source is stable. To radiate these modes effectively, the converter introduced in this part is mainly to realize the mode conversion from TEM to TE_{11} coaxial waveguide mode (Coa.TE_{11}) at low band and TM_{01} to TE_{11} circular waveguide mode (Cir.TE_{11}) at high band.

The TEM-TE_{11} converter (Yuan *et al.*, 2005), with a coaxial plate-inserted structure, has the virtues of co-aligned ports, a compact structure, and easy manufacturing. Such a converter also can be designed to transform the TM_{01} mode into the TE_{11} mode, with a simple TM_{01} $-$ TEM converter (a nose on the inner conductor) being embodied in it. Considering its special structure, it can also be redesigned with a TM_{01} $-$ TE_{11} converter at high band being inserted properly in a TEM-TE_{11} converter at low band, as shown in Figure 2. We have designed such a dual-band feed line with co-aligned ports at 1.75 GHz and 4.15 GHz.

The length of the total structure is 33 cm. It has a conversion efficiency of 97.1% at 1.75 GHz and 98.7% at 4.15 GHz, respectively. If 90% of mode conversion to the TE_{11} mode is acceptable, the bandwidth ($\Delta f/f_0$) for conversion efficiency $>$90% is 10.3% (1.69–1.87 GHz) and 9.9% (4.01–4.42 GHz), respectively. The conversion efficiencies are shown in Figures 3 and 4, as a function of frequency. On the other hand, there is no electric field concentrating at the edges of the plates, and the inserted plates will not reduce the power-handling capacity obviously, which can also be confirmed by numerical simulation. In the simulation, the input power is 1.0 Watt, and the electric field strength is less than 10.43 V/cm and 12.23 V/cm, respectively. Generally, the mode converter is usually pumped into high vacuum state (less than 10^{-2} Pa), in which the electric field breakdown threshold is greater than 1.0 MV/cm at short microwave duration (most of the modern HPM durations are less than 100 ns). So it can be estimated that the power handling capacity reaches 9.19 GW at 1.75 GHz and 6.69 GW at 4.15GHz, respectively (Baker & Schamiloglu, 2001).

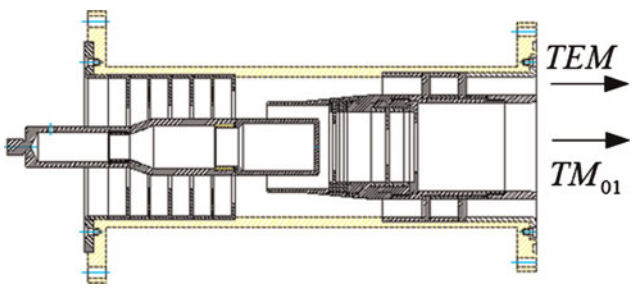

Fig. 1. (Color online) Cross-section of a novel coaxial dual-band HPM source.

https://doi.org/10.1017/S0263034610000327 Published online by Cambridge University Press

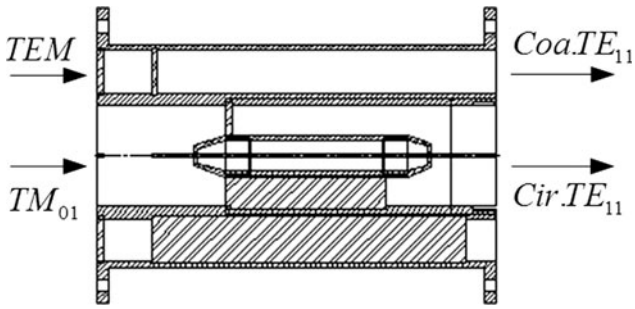

Fig. 2. Schematic of dual-band mode converter with co-aligned ports.

Dual-Band Feed Line with Off-Aligned Input Ports and Coaxial Output Ports

Many HPM sources working at single-band have been designed successfully, generating azimuthally symmetric output modes (TM_{01} circular waveguide mode etc.). The representative ones are virtual cathode oscillators (VIRCATORs) (Belomyttsev *et al.*, 2003; Sze *et al.*, 1987), backward wave oscillators (Korovin *et al.*, 2003), magnetically insulated transmission line oscillators (MILOs) (Lemke *et al.*, 1997), cherenkov generator, and so on. Our laboratory also have done much research on VIRCATORs (Li *et al.*, 2008) and MILOs (Fan *et al.*, 2007), providing well performance HPM sources. Taking VIRCATORs and MILOs for example, the stable operation frequencies are 4.15 GHz and 1.75 GHz, respectively. Then another type of dual-band power combining architecture is shown in Figure 5, and the feed line to be designed is part 3 in this figure. It is not only for realizing the conversion from TM_{01} to TE_{11} at dual-band, but also realizing superposition of axis of the two separate radiation systems (Zhang *et al.*, 2010).

This feed line consists of two structures, and the first structure is a serpentine metal pipe with circular cross section and serpentine curved axis in one plane, as shown in Figure 6, which is comprised of a straight waveguide with length L

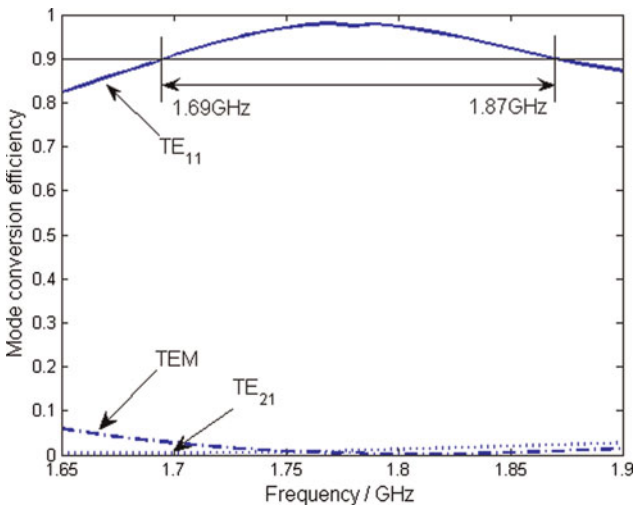

Fig. 3. (Color online) Mode conversion efficiency of TEM-$Coa.TE_{11}$ as a function of frequency.

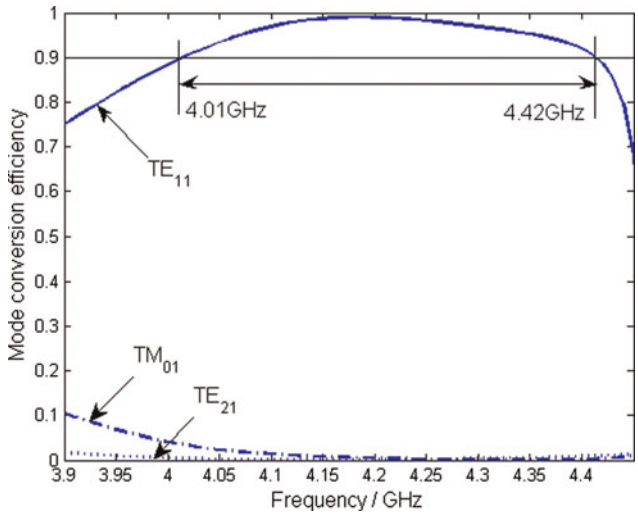

Fig. 4. (Color online) Mode conversion efficiency of TM_{01}-$Cir.TE_{11}$ as a function of frequency.

and two bent waveguides with curvature radius R_1 and $-R_2$, and bend angles θ, respectively, where, the minus symbol represents the second bent waveguide is opposite to the first one.

The method of simulating mode conversion in a serpentine converter is outlined based on the coupling equations (Morgan, 1957; Thumm, 1984, 1986), and mode conversions due to curvature in circular waveguides have been systematically studied (Li & Thumm, 1991). If the axis of the first source offsets Δx with the primary axis, sometimes the straight waveguide with length L plays an important part in meeting this requirement, then the objective function can be written as

$$\begin{cases} R_1(1-\cos\theta) - R_2(1-\cos\theta) + L\sin\theta = \Delta x \\ \eta = 1 \end{cases}, \quad (1)$$

where η is mode conversion efficiency from TM_{01} to TE_{11} mode.

For the application at operation frequency $f_0 = 4.15$ GHz, the authors wrote a general optimizing code (Yuan & Zhang, 2009), in which the conversion efficiency was chosen as the maximum objective function, and the geometrical characteristics of the mode converter were chosen as free parameters (under certain offset Δx) to be optimized. The mode conversion efficiency and the other parameters, as a function of axis offset are given in Table 1, which indicates that the results meet the requirements of the objective function.

Taking $\Delta x = 20$ cm for example, it has a conversion efficiency of 99.52% at 4.15 GHz, and the bandwidth ($\Delta f/f_0$) for conversion efficiency >90% is 25.54% (3.57–4.63 GHz). The conversion efficiencies are shown in Figure 7, as a function of frequency. On the other hand, there is no electric field concentrating in the dual-bend circular waveguide, which can not reduce the power-handling capacity obviously, as shown in Figure 8. It is observed that the TM_{01} mode

https://doi.org/10.1017/S0263034610000327 Published online by Cambridge University Press

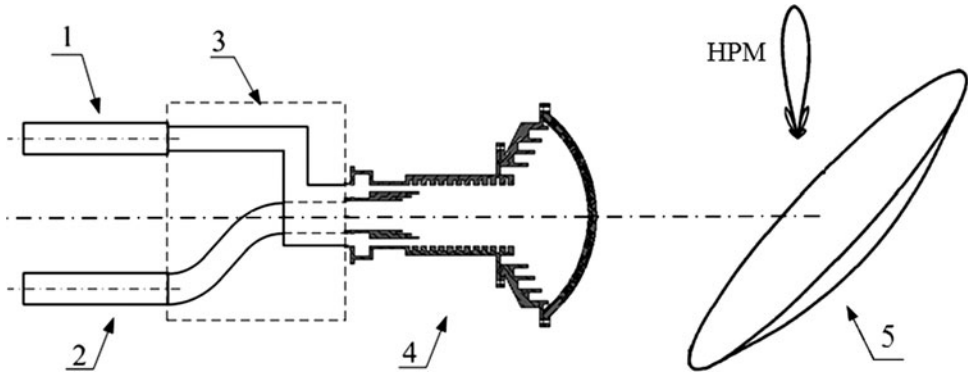

Fig. 5. Structure of dual-band incoherent power combining system, and the dual-band microwave is generated by two separate sources. Part 1and 2 stand for MILOs and VIRCATORs, parts 3 and 4 denote the feed line and dual-band horn feed to be designed, respectively. Part 5, paraboloidal main reflector, is an offset-shaped single-reflector antenna.

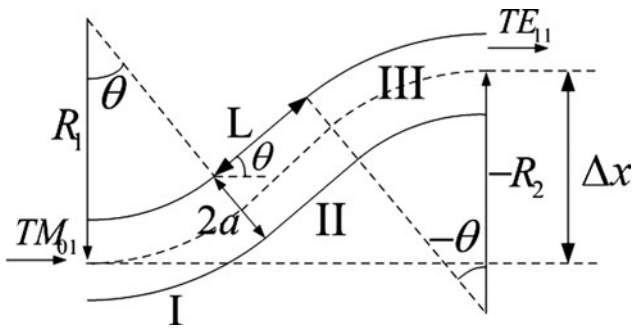

Fig. 6. Structure of the dual-bend circular waveguide mode converter.

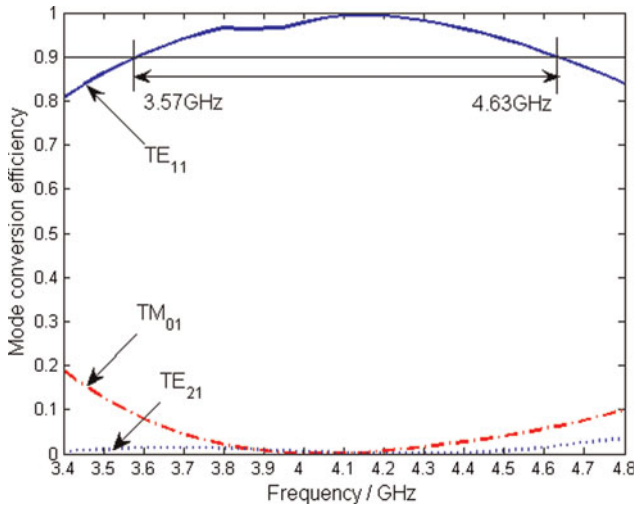

Fig. 7. (Color online) Mode conversion efficiency of TM_{01}-TE_{11} as a function of frequency.

propagates in the mode converter has been converted into TE_{11} mode while passing through the converter. And according to the simulation, the power handling capacity reaches up to 10 GW at 4.15 GHz if the threshold of microwave breakdown is 1 MV/cm in the vacuum state (Baker & Schamiloglu, 2001).

The second structure is a combined converter, consisting of a TM_{01}-TE_{10} converter, a TE_{10} transmission line and a TE_{10}-TE_{11} converter, as shown in Figure 9. We have designed such a converter at 1.75 GHz. The design of input port should reduce the return loss of TM_{01} circular waveguide mode as much as possible, with a nose being embodied on the inner conductor. And the inner radius of circular waveguide, locating at the input port, was designed with $R = 7.0$ cm to restrain return loss of high order modes. The design of TE_{10} transmission line should avoid the stimulation of high order modes, due to the bend of rectangular waveguide. The distance L_4 between input and output ports can

Table 1. *Structure of dual-bend converter and its simulation results*

Δx (cm)	a (cm)	L (cm)	R_1 (cm)	R_2 (cm)	θ (deg)	Conversion efficiency	
						Theoretical (%)	Simulated (%)
9	3.20	0.00	9.56	9.56	58.03	99.7	99.46
12	3.50	0.00	14.09	14.09	54.94	99.8	99.88
15	3.90	0.00	21.24	21.24	49.69	99.9	98.94
17	4.20	0.00	27.93	27.93	45.92	99.8	99.24
20	4.80	12.87	33.88	40.89	34.02	99.5	99.52
50	3.72	47.63	22.52	14.45	50.30	99.6	99.50

https://doi.org/10.1017/S0263034610000327 Published online by Cambridge University Press

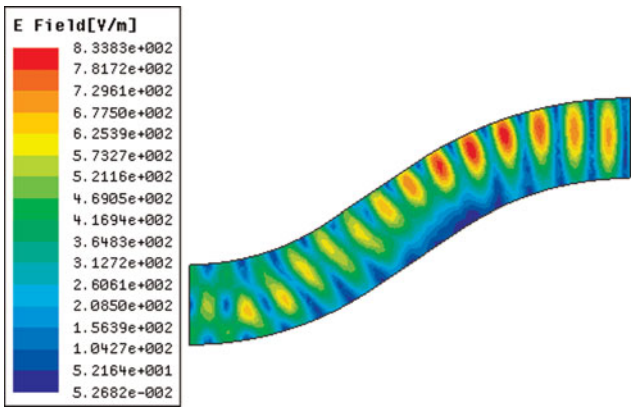

Fig. 8. (Color online) E-field distribution of the dual-bend mode converter.

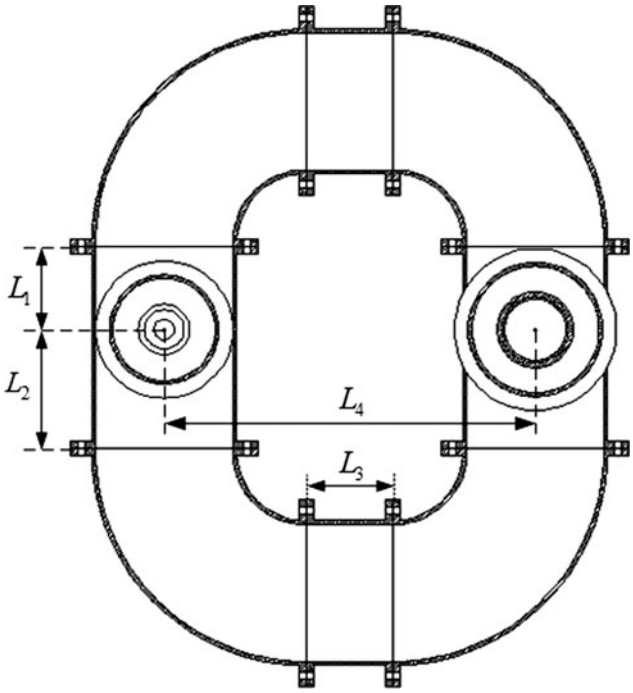

Fig. 9. The whole geometrical structure of Cir.TM_{01}-Coa.TE_{11} mode converter based on intermediate TE_{10} rectangular waveguide mode.

be changed to meet the requirements in some special applications by adjusting the length L_3. Two TE_{10} rectangular waveguide modes can be interchanged into TE_{11} coaxial waveguide mode under the condition that the two TE_{10} modes' phase difference is odd times of π, based on coaxial waveguide theory. In this structure, the guide wavelength of the TE_{10} mode is 192.44 mm, and the two TE_{10} modes' phase difference can meet the requirement of odd times of π, only if $L_2 - L_1 = \lambda_g/4 = 48.11$ mm.

Based on the above analysis, this combined mode converter has been investigated in detail. Figure 10 denotes that the input TM_{01} circular waveguide mode has been successfully converted into TE_{11} coaxial output mode, and Figure 11 displays the conversion efficiencies of the TM_{01}-TE_{10} converter, the TE_{10} transmission line, the TE_{10}-TE_{11} converter, and the total TM_{01}-TE_{10}-TE_{11} converter *versus* frequency. The overall transmission efficiency of TM_{01}-TE_{10}-TE_{11} at center frequency is 98.5%, and the bandwidth for $\eta > 90\%$ is about 10%. Obviously, reducing reflection loss of TM_{01} mode is an effective approach to widen the bandwidth. However, it can still meet our requirements based on the well performance HPM sources. According to the simulation, the electric field strength is less than 10.31 V/cm if the input power is 1.0 Watt, and it can be estimated that the power handling capacity reaches 9.40 GW at 1.75 GHz if the threshold of microwave breakdown is 1 MV/cm in the vacuum state (Baker & Schamiloglu, 2001).

DEGIGN OF DUAL-BAND HORN FEED AND PERFORMANCE

Compared with conversional corrugated horns, horn antennas that combine horizontal and vertical corrugations are apparently easier to manufacture and they also have high performances in a compact size (Teniente *et al.*, 2002, 2006). We have also described a dual-band horn feed with this type of corrugations in this paper, which has a high power handling capacity (Zhang *et al.*, 2009). The horn feed can be used to radiate HPMs with a good far-field radiation pattern at each band, and thus one reflection antenna can

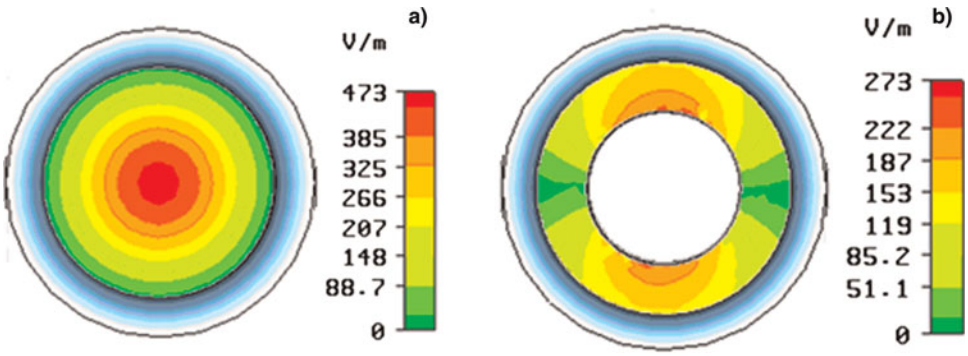

Fig. 10. (Color online) E-field distribution of the input and output mode. (**a**) input TM_{01} circular waveguide mode; (**b**) output TE_{11} coaxial waveguide mode.

https://doi.org/10.1017/S0263034610000327 Published online by Cambridge University Press

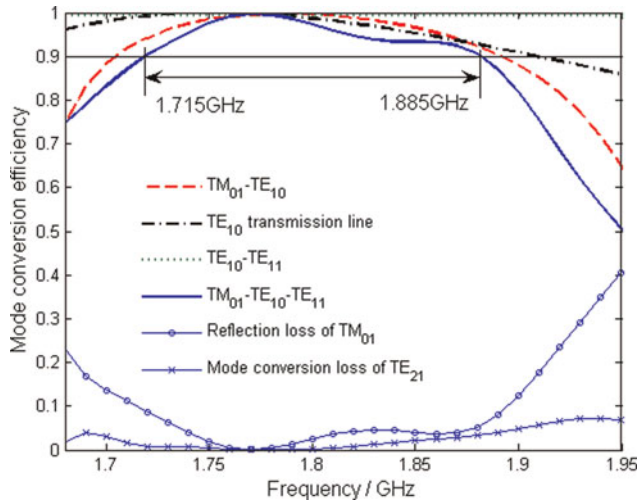

Fig. 11. (Color online) Transmission efficiency of TM_{01}-TE_{10} converter, the TE_{10} transmission line, the TE_{10}-TE_{11} converter and the total TM_{01}-TE_{10}-TE_{11} converter. Return loss of TM_{01} mode could be optimized to improve the bandwidth, if needed.

be utilized effectively to radiate dual-band microwaves. In addition, the horn feed is simple to manufacture.

The horn feed, consisting of a series of discontinuities, is fed by a coaxial waveguide at L-band and a circular waveguide at C-band. And the coaxial and circular waveguides are stimulated by the dominant TE_{11} mode and connected to the corrugated section as shown in Figure 12. Considering its special structure, TE_{1n} and TM_{1n} modes can be excited at each discontinuity in the feed. Mode matching theory is an effective approach to obtain the overall scatter matrix from which to determine the propagation properties of the feed, progressively cascading the scatter matrix of each discontinuity in cross section and each of the short lengths of waveguide in isolation (James, 1981; James & Thomas, 1982). The analysis allows the return loss and

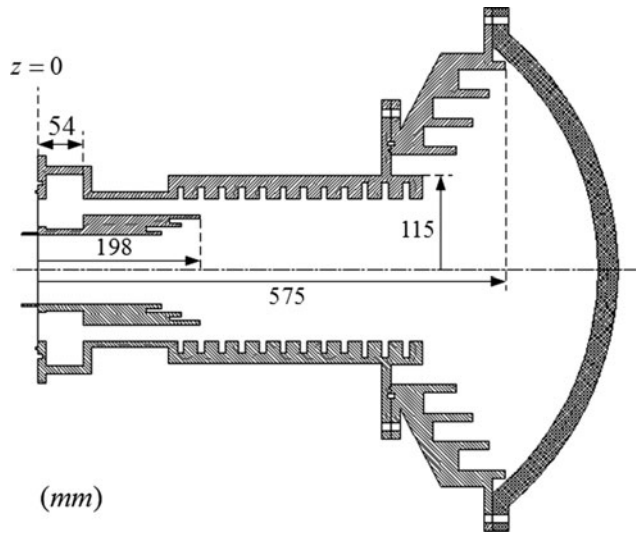

Fig. 12. Cross-section of coaxial dual-band horn feed.

transmission coefficient of each band to be computed accurately. Using mode expansion technology, we can get the far-field radiation pattern of the feed. And radiation pattern can be written as

$$F_\theta(\theta,\varphi)=\cos\varphi\left[\sum_{m=1}^{\infty}\frac{S_{21}(m,1)}{\sqrt{P_{TE_{1m}}}}\frac{ikd^2}{2}\frac{J_1(v_m)}{v_m}\times\left(1+\beta_m/k\cos\theta\right)\frac{J_1(kd\sin\theta)}{kd\sin\theta}\frac{e^{-ikR}}{R}+\sum_{n=1}^{\infty}\frac{S_{21}(n,1)}{\sqrt{P_{TM_{1n}}}}\frac{-ikd^2}{2}\frac{J_1'(\mu_n)}{(\mu_n/kda\sin\theta)^2-1}\times\left(1+k/\beta_n\cos\theta\right)\frac{J_1(kd\sin\theta)}{kd\sin\theta}\frac{e^{-ikR}}{R}\right],\tag{2}$$

$$F_\varphi(\theta,\varphi)=\sin\varphi\sum_{m=1}^{\infty}\frac{S_{21}(m,1)}{\sqrt{P_{TE_{1m}}}}\frac{ikd^2}{2}\frac{J_1(v_m)}{v_m}\times\left(\cos\theta+\beta_m/k\right)\frac{J_1'(kd\sin\theta)}{1-\left(kd\sin\theta/v_m\right)^2}\frac{e^{-ikR}}{R},\tag{3}$$

where, v_m and μ_n are the roots of the Bessel equation J_1 and J_1', respectively, d is the aperture radius, β_m and β_n denote propagation constant of TE_{1m} mode and TM_{1n} mode at the aperture, respectively. $S_{21}(m,1)$ and $S_{21}(n,1)$ represent the complex transmission coefficients obtained by mode matching theory. By using Eqs. (2) and (3), one can obtain E-plane and H-plane radiation pattern under the condition of $\varphi=0^\circ$ and $\varphi=90^\circ$, respectively.

As mentioned above, this method can avoid solving the (complex) roots of the feed's characteristic equation, thus it is convenient to optimize the whole structure of the feed. The whole structure is divided into three parts to avoid using a great deal of time and a large mount of memory for simulation. First, the inner choke horn is designed to be flare angle controlled (Ying *et al.*, 1995), and the depth and width of coaxial corrugations are chosen as free parameters to be optimized to reduce the diffraction from the inner horn edge. Second, a circular waveguide with vertical corrugations plays an important part in the dual-band feed. Assuming the inner radius of the circular waveguide is a and the wavelength at 1.75 GHz is λ, under the condition of $1.6398\,a<\lambda$, higher order modes at low frequency stimulated at the aperture of the inner horn can be prohibited effectively. On the other hand, circular waveguide with vertical corrugations is equal to a TE_{11}-to-HE_{11} mode converter at high frequency. Finally, the outer choke horn is designed in the same way as the inner choke horn to improve azimuthally symmetric output modes at low frequency, and it should avoid influencing the radiation pattern at high frequency simultaneously. To improve the power handling capacity of the feed, four coaxial corrugations are chosen to decrease the electric field strength at the aperture.

Dozens of different geometries have been analyzed to reach the final design, with the dimensions given in Table 2 and

https://doi.org/10.1017/S0263034610000327 Published online by Cambridge University Press

Table 2. *Dimensions of the dual-band horn feed*

Parts	Parameters in common	Corrugation number (from throat to aperture)	Depth (mm)	z-location of top of ridges (mm)
Inner horn with horizontal corrugations	$d_1 = 5$ mm	1	18	150
	$d_2 = 5$ mm	2	15	175
Circular waveguide with vertical corrugations	$d_1 = 8$ mm	1–9	16	None
	$d_2 = 17$ mm	10–12	18	None
Outer horn with horizontal corrugations	$d_1 = 10$ mm	1	30	470
	$d_2 = 25$ mm	2	40	515
		3	40	535
		4	41	555

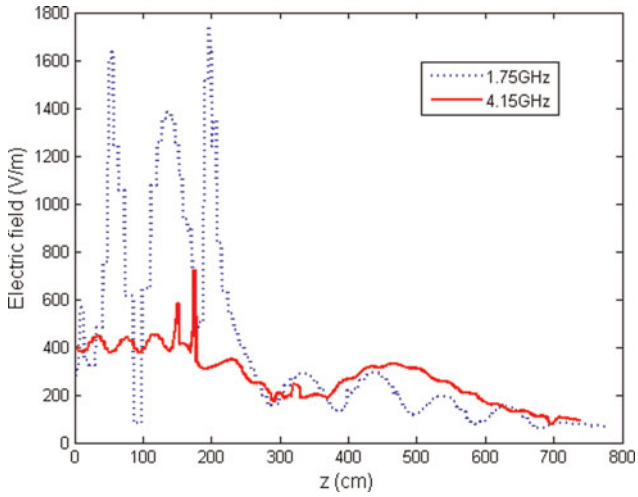

Fig. 14. (Color online) Electric field along the axial (input power is 1 W).

Figure 12, where the width of corrugations is d_1 and the thickness of ridges between them is d_2. Generally, the horn feed is always pumped into high vacuum state (less than 10^{-2} Pa) in application, and a spherical cover is utilized to airproof the horn feed. At last, the whole system structure is less than $\Phi 75$ cm $\times$ 60 cm.

The E-plane and H-plane of feed patterns at 1.75 GHz and 4.15 GHz are shown in Figure 13. Relative to the maximum gain possible, the L-band transmit gain is only lower by 0.5 dB than C-band. It is observed that E-plane and H-plane patterns of the feed are almost equal to each other in the illuminated area, while the feed is applied as a primary feed in an offset-shaped single-reflector antenna system. The power-handling capacity of the horn feed was also estimated by calculating the electric field strength on the axis of the feed, which is shown in Figure 14. According to the simulation, the input power is 1.0 Watt, and the origin of the z-axis is at the junction of the feed and mode converter. In the whole structure, the electric field strength is less than 17.34 V/cm at 1.75 GHz and 7.84 V/cm at 4.15 GHz, respectively. So it can be estimated that the power handling capacity in the horn feed reaches 3.33 GW at 1.75 GHz and 10 GW at 4.15 GHz, respectively (Baker & Schamiloglu, 2001). In the near field, the electric field strength is less than 1.05 V/cm, and the breakdown threshold in atmosphere under the condition of short microwave duration is about 5×10^4 V/cm, so the power breakdown threshold in this area is about $(5 \times 10^4/1.05)^2 = 2.3$ GW. It means that the antenna breakdown will take place in the near field of the antenna. The power-handling capacity of the dual-band horn feed is about 2.3 GW.

The L-band and C-band return loss is shown in Figure 15. A simple discontinuity designed in coaxial waveguide was used to produce better than a -20 dB return loss at 1.75 GHz.

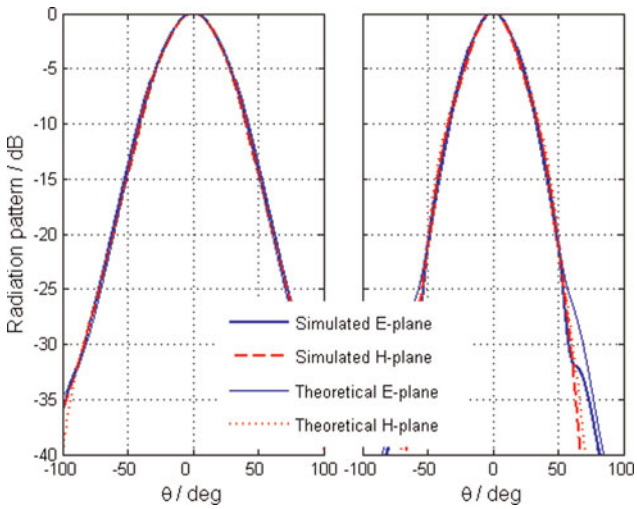

Fig. 13. (Color online) E- and H-plane feed patterns at 1.75 GHz (left) and 4.15GHz (right).

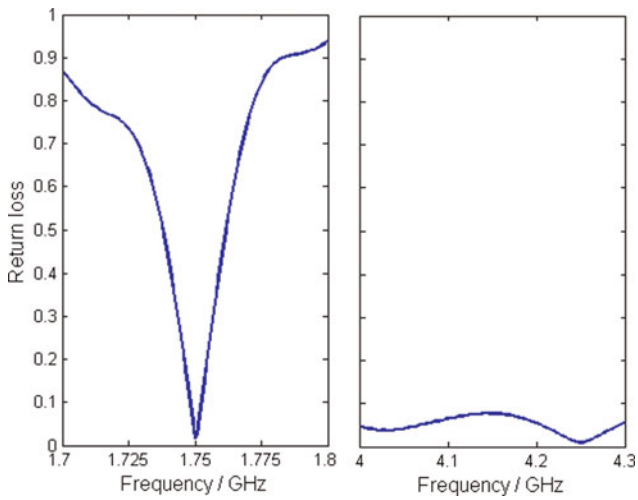

Fig. 15. (Color online) L-band (left) and C-band (right) return loss as a function of frequency.

https://doi.org/10.1017/S0263034610000327 Published online by Cambridge University Press

If necessary, a more sophisticated matching technique could be used to improve the bandwidths. Around the operation frequency 4.15 GHz, return loss is better than −20 dB. Furthermore, the phase center of each band has been calculated from the radiation field, and it is located within $z = 44.5 \pm 2.0$ cm over the dual-band. It can be seen that the performance levels achieved by this new design technique are fairly high, which is especially significant for the higher performance of horn feeds in dual- or multi-band HPM applications.

CONCLUSIONS

This paper has presented a complete study of a novel incoherent power combining architecture including a dual-band horn feed and two feed line structures. It has shown that the azimuthally symmetric output modes (the TM_{01} circular waveguide mode and the TEM coaxial waveguide mode) can be interchanged effectively through the two feed lines, and a good far-field radiation pattern of each band has been achieved. Two types of feed lines have a similar conversion efficiency of about 98% and a bandwidth of about 10%, at 1.75 GHz and 4.15 GHz, respectively. Although bandwidth of the dual-band horn feed at L-band is not very good, it still provides an efficient approach to realize incoherent power combining of HPM sources. In addition, the radiation system is large enough for high power handling capacity, and experimental research is planned for the next step in order to make sure the sufficient power handling capacity. A more sophisticated matching technique need to be studied to improve the reflection characteristic of L-band. More detailed measurements and refinements in the operation of the architecture are on going, and future research includes the multi-band horn feed and theoretical design of feed lines with a high power handling capacity, according with the development trends of HPM technology.

ACKNOWLEDGMENTS

This work was supported by the National High Technology Research and Development Program of China. The authors wish to express gratitude to L. M. Li and H. J. Zhou for their discussions and help in revising the manuscript.

REFERENCES

Baker, R.J. & Schamiloglu, E. (2001). *High-Power Microwave Sources and Technologies*. New York: The Institute of Electrical and Electronics Engineers, Inc.

Belomyttsev, S.Y., Grishkov, A.A., Korovin, S.D. & Ryzhov, V.V. (2003). On the current of an annular electron beam with a virtual cathode in a drift tube. *Laser Part. Beams* **21**, 561–565.

Benford, J., Swegle, J.A. & Schamiloglu, E. (2007). *High Power Microwaves-2nd ed.* New York & London: Taylor & Francis Group.

Eltchaninov, A.A., Korovin, S.D., Rostov, V.V., Pegel, I.V., Mesyats, G.A., Rukin, S.N., Shpak, V.G., Yalandin, M.I. & Ginzburg, N.S. (2003). Production of short microwave pulses with a peak power exceeding the driving electron beam power. *Laser Part. Beams* **21**, 187–196.

Fan, Y.W., Yuan, C.W., Zhong, H.H., Shu, T., Zhang, J.D., Yang, J.H., Yang, H.W., Wang, Y. & Luo, L. (2007). Experimental Investigation of an Improved MILO. *IEEE Trans. on Plasma Sci*. **35**, 1075–1080.

Fan, Y.W., Zhong, H.H., Li, Z.Q., Shu, T., Zhang, J.D., Zhang, J., Zhang, X.P., Yang, J.H. & Luo, L. (2007). A double-band high-power microwave source. *Journal of Applied Physics* **102**.

Flodin, J., Kildal, P.S. & Kishk, A. (1996). Moment Method Design of a Large S/X Band Corrugated Horn. Antennas and Propagation Society International Symposium **3**, 2030–2033.

Imbriale, W.A. (2005). An alternative feed design for the MRO antenna. *IEEE Trans. Antennas Propag*. **5**, 761–764.

James, G.L. (1981). Analysis and Design of TE_{11}-to-HE_{11} Corrugated Cylindrical Waveguide Mode Converters. *IEEE Trans. on Microwave Theory and Techniques* **29**, 1059–1066.

James, G.L. & Thomas, B.M. (1982). TE_{11} to HE_{11} Cylindrical Waveguide Mode Converters Using Ring-Loaded Slots. *IEEE Trans. on Microwave Theory and Techniques* **30**, 278–285.

Korovin, S.D., Kurkan, I.K., Loginov, S.V., Pegel, I.V., Polevin, S.D., Volkov, S.N. & Zherlitsyn, A.A. (2003). Decimeter-band frequency-tunable sources of high-power microwave pulses. *Laser Part. Beams* **21**, 175–185.

Lemke, R.W., Calico, S.E. & Clark, M.C. (1997). Investigation of a load-limited magnetically insulated transmission line oscillator (MILO). *IEEE Trans. Plasma Sci*. **25**, 364–374.

Li, G.L., Yuan, C.W., Zhang, J.Y., Shu, T. & Zhang, J. (2008). A diplexer for gigawatt class high power microwaves. *Laser Part. Beams* **26**, 371–377.

Li, H. & Thumm, M. (1991). Mode conversion due to curvature in corrugated waveguides. *Int. J. Electron*. **71**, 333–347.

Li, L., Liu, L., Cheng, G., Chang, L., Wan, H. & Wen, J. (2009*a*). Electrical explosion process and amorphous structure of carbon fibers under high-density current pulse igniting intense electron-beam accelerator. *Laser Part. Beams* **27**, 511–520.

Li, L., Liu, L., Cheng, G., Xu, Q., Ge, X. & Wen, J. (2009*b*). Layer structure, plasma jet, and thermal dynamics of Cu target irradiated by relativistic pulsed electron beam. *Laser Part. Beams* **27**, 497–509.

Li, L., Liu, L., Xu, Q., Chen, G., Chang, L., Wan, H. & Wen, J. (2009*c*). Relativistic electron beam source with uniform high-density emitters by pulsed power generators. *Laser Part. Beams* **27**, 335–344.

Li, Z.Q., Zhong, H.H., Fan, Y.W., Shu, T., Yang, J.H., Yuan, C.W., Xu, L.R. & Zhao, Y.S. (2008). Simulation and Experimental Research of a Novel Vircator. *Chin. Phys. Lett*. **25**, 2566–2568.

Liu, J.L., Cheng, X.B., Qian, B.L., Ge, B., Zhang, J.D. & Wang, X.X. (2009). Study on strip spiral Blumlein line for the pulsed forming line of intense electron-beam accelerators. *Laser Part. Beams* **27**, 95–102.

Liu, J.L., Li, C.L., Zhang, J.D., Li, S.Z. & Wang, X.X. (2006). A spiral strip transformer type electron-beam accelerator. *Laser Part. Beams* **24**, 355–358.

Liu, J.L., Yin, Y., Ge, B., Zhan, T.W., Chen, X.B., Feng, J.H., Shu, T., Zhang, J.D. & Wang, X.X. (2007*a*). An electron-beam accelerator based on spiral water PFL. *Laser Part. Beams* **25**, 593–599.

Liu, J.L., Zhan, T.W., Zhang, J., Liu, Z.X., Feng, J.H., Shu, T., Zhang, J.D. & Wang, X.X. (2007*b*). A Tesla pulse transformer for spiral water pulse forming line charging. *Laser Part. Beams* **25**, 305–312.

Liu, R., Zou, X., Wang, X., He, L. & Zeng, N. (2008). X-pinch experiments with pulsed power generator (PPG-1) at Tsinghua University. *Laser Part. Beams* **26**, 33–36.

Morgan, S.P. (1957). Theory of curved circular waveguide containing an inhomogeneous dielectric. *Bell Syst. J*. 1209–1251.

Sze, H., Benford, J. & Woo, W. (1987). High-power microwave emission from a virtual cathode oscillator. *Laser Part. Beams* **5**, 675–681.

Teniente, J., Goñi, D., Gonzalo, R. & del-Río, C. (2002). Choked Gaussian Antenna: Extremely Low Sidelobe Compact Antenna Design. *IEEE Antennas and Wireless Propag. Lett*. **1**, 200–202.

Teniente, J., Gonzalo, R. & del-Río, C. (2006). Innovative High-Gain Corrugated Horn Antenna Combining Horizontal and Vertical Corrugations. *IEEE Antennas and Wireless Propag. Lett*. **5**, 380–383.

Thumm, M. (1984). High Power Millimetre-Wave Mode Converters in Overmoded Circular Waveguides using Periodic Wall Perturbations. *Int. J. Electronics* **57**, 1225–1246.

Thumm, M. (1986). High Power Mode Conversion for Linearly Polarized HE_{11} Hybrid Mode Output. *Int. J. Electronics* **61**, 1135–1153.

Vardaxoglou, J.C., Seager, R.D. & Robinson, A.J. (1992). Novel 'soft' horn antenna for multiband operation. *IEE Colloquium on Multi-Band Antennas*.

Yang, S. & Li, H.F. (1997). Optimization of novel high-power millimeter-wave TM_{01}-TE_{11} mode converters. *IEEE Trans. on Microwave Theory and Techniques* **45**, 552–554.

Yatsui, K., Shimiya, K., Masugata, K., Shigeta, M. & Shibata, K. (2005). Characteristics of pulsed power generator by versatile inductive voltage adder. *Laser Part. Beams* **23**, 573–581.

Ying, Z., Kishk, A.A. & Kidal, P.S. (1995). Broadband compact horn feed for prime-focus reflectors. *Electronics Lett*. **31**, 1114–1115.

Yuan, C.W., Liu, Q.X., Zhong, H.H. & Qian, B.L. (2005). A novel TEM-TE_{11} mode converter. *IEEE Microw. Wireless Component Lett*. **15**, 513–515.

Yuan, C.W. & Zhang, Q. (2009). Design of a TM_{01}-TE_{11} Transmission Line for High-Power Microwave Applications. *IEEE Trans. on Plasma Sci*. **37**, 1908–1915.

Zhang, Q., Yuan, C.W. & Liu, L. (2009). A Coaxial Corrugated Dual-band Horn Feed. *IEEE Antennas Wireless Propag. Lett*. **8**, 1357–1359.

Zhang, Q., Yuan, C.W. & Liu, L. (2010). Design of a coaxial radiation feeder structure applied in dual-band feed. *High Power Laser and Particle Beams* **22**, 1107–1111.

Zhang, X.P., Wang, T., Li, Z.Q., Liu, J., Qian, B.L. & Zhang, J.D. (2008). Preliminary experimental studies of a dual-band HPM source. Lijiang: Proceedings of the 11th State Conference on High-power Particle Beams.

Zou, X.B., Liu, R., Zeng, N.G., Han, M., Yuan, J.Q., Wang, X.X. & Zhang, G.X. (2006). A pulsed power generator for x-pinch experiments. *Laser Part. Beams* **24**, 503–509.

https://doi.org/10.1017/S0263034610000327 Published online by Cambridge University Press